J Electroceram (2010) 25:26–37
DOI 10.1007/s10832-009-9585-8

Anisotropic piezoelectric properties of 1–3 ceramic / polymer composites comprising rods with elliptic cross section

V. Yu. Topolov · P. Bisegna

Received: 7 October 2008 / Accepted: 20 July 2009 / Published online: 8 August 2009

Abstract This paper is concerned with the study of effective piezoelectric properties of 1–3 ferroelectric ceramic / polymer composites. The aim of this paper is to show the role of a combination of the electromechanical properties of components and microgeometry of the 1–3 composite in determining its anisotropic piezoelectric response. The system of ceramic rods in the form of elliptic cylinders is an important microgeometric factor that influences the piezoelectric coefficients and their anisotropy. Examples of the piezoelectric response and anisotropy are analysed for the 1–3 composites based on either "soft" or "hard" ceramic and having either piezo-active or piezo-passive matrix. Combinations of the ceramic and polymer components are found that provide different volume-fraction dependences of the piezoelectric coefficients d_{3j}^* and g_{3j}^*: both monotonic, both non-monotonic, monotonic d_{3j}^* and non-monotonic g_{3j}^*, and *vice versa*. Examples of volume-fraction dependences of electromechanical coupling factors k_{3j}^* are also considered. A comparison of the effective piezoelectric coefficients calculated by the effective field method and the finite element method is carried out for different compositions in wide ranges of the ratio of semiaxes of the ellipse and of volume fractions of the components. Good agreement between data calculated by means of the aforementioned methods is obtained for the 1–3 structure comprising the elliptic cylinders.

V. Yu. Topolov (✉)
Department of Physics, Southern Federal University,
5 Zorge Street,
344090 Rostov-on-Don, Russia
e-mail: vutopolov@sfedu.ru

V. Yu. Topolov · P. Bisegna
Department of Civil Engineering,
University of Rome "Tor Vergata",
00133 Rome, Italy

Keywords Electromechanical properties · Piezoelectric coefficients · 1–3 piezo-active composite · Effective field method · Finite element method

Pacs 77.84.-s · 77.84.Lf · 77.65.-j · 77.65.Bn · 77.90.+k · 43.38.Fx

1 Introduction

Piezo-active composites based on ferroelectric ceramics (FCs) are of practical interest due to various effective electromechanical properties, considerable electromechanical coupling factors, figures of merit, and other parameters [1–5]. Composites with connectivity 1–3 (in terms of the widespread classification by Newnham et al. [6]) represent the vast group of advanced materials [1–3] that contain a system of long FC rods, connected in one direction and surrounded by a continuous polymer matrix (connected in three directions). As a consequence, the effective parameters of the 1–3 FC / polymer composite considerably depend [2–5, 7] on microgeometric features, electromechanical properties and volume fractions of the components, poling conditions, *etc*. The effective electromechanical properties were predicted and analysed for the 1–3 composites with the FC rods having the following cross section: circle [2, 8–12], square [7, 13–16], rectangle [17], ellipse [14, 18], octagon [14], and cross [14]. Among FC components in the 1–3 composites one can mention compositions based on Pb(Zr, Ti)O_3 (PZT-type) [2–5, 7–11, 14–16] or Pb(Ca, Ti)O_3 [7, 12, 15]. A transition from a transversely isotropic composite to an anisotropic one was considered in paper [11] where 36 classes of the piezo-active 1–3 composites were introduced. Very recently, the effect of the rod shape on the effective electromechanical properties was studied for the 1–3

"longitudinal" and "transverse" composites with elastically anisotropic and piezoelectrically active components [14]. However, the anisotropic piezo-active composites comprising rods with elliptic cross section were not yet considered in detail, especially for different combinations of the FC and polymer components. Our present work is devoted to the study on the 1–3 FC / polymer composites in which the FC rods in the form of an elliptic cylinder influence the piezoelectric properties and their anisotropy in different ways. The aim of this paper is to show the role of a combination of the electromechanical properties of components and microgeometry of the 1–3 composite in determining its anisotropic piezoelectric response and electromechanical coupling.

2 Modelling of effective electromechanical properties of composites

According to our model, the 1–3 composite has a cellular structure and a regular distribution of the FC rods in the polymer matrix. Cross sections of these rods by the X_1OX_2 plane of the rectangular co-ordinate system $(X_1X_2X_3)$ (Fig. 1) are described by

$$(x_1/a_1)^2+(x_2/a_2)^2=1. \tag{1}$$

Equation (1) is relative to the axes of the co-ordinate system $(X_1X_2X_3)$. Semi-axes of the ellipse a_f (f=1 and 2) from Eq. (1) are constant in the whole composite sample. Centres of symmetry of these ellipses are arranged periodically on the OX_1 and OX_2 directions (Fig. 1). It is assumed that all the rods are aligned along the OX_3 axis and the height of each rod obeys condition $h>>a_f$. Manufacturing the studied FC / polymer composite with the appointed microgeometry can be based on the rapid prototyping method that provides the fabrication flexibility in achieving the structural complexity and hierarchy in piezo-active composites [19].

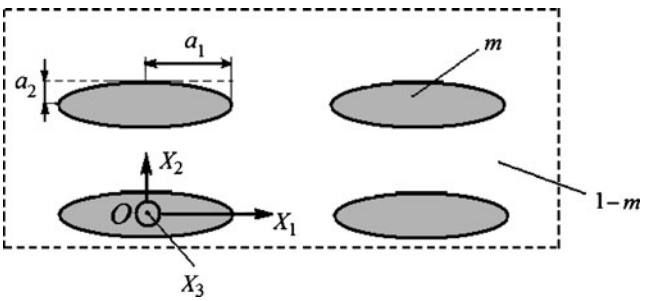

Fig. 1 Cross section of the 1–3 FC / polymer composite by the X_1OX_2 plane. $(X_1X_2X_3)$ is the rectangular co-ordinate system, a_1 and a_2 are semiaxes of the ellipse, m is the volume fraction of FC, and $1-m$ is the volume fraction of polymer

The remanent polarisation vector of each FC rod is $\boldsymbol{P_r}^{(1)} \uparrow\uparrow OX_3$. The polymer matrix can be either ferroelectric (piezo-active in the poled state) with the remanent polarisation vector $\boldsymbol{P_r}^{(2)}$ or simply dielectric (piezo-passive) with $\boldsymbol{P_r}^{(2)}=\boldsymbol{0}$. Taking into account considerable difference between coercive fields of the FC and ferroelectric polymer components (see, *e.g.*, Refs. 20, 21), one can manufacture composites with $\boldsymbol{P_r}^{(2)} \uparrow\uparrow OX_3$, $\boldsymbol{P_r}^{(2)} \uparrow\downarrow OX_3$ or other $\boldsymbol{P_r}^{(2)}$ orientations in the polymer matrix.

The effective electromechanical properties of the 1–3 composite are determined in a long-wave approximation. It means that sizes of FC grains are much smaller than the shorter axis $2a_2$ of the ellipse from Eq. (1). Moreover, wavelengths of waves being propagated from acoustic radiators are assumed to be much longer than the height h of the rod and the composite sample as a whole. The following constants $X^{(n)}$ of the components are used for calculations: elastic moduli $c_{ab}^{(n),E}$ measured at electric field E = const, piezoelectric coefficients $e_{ij}^{(n)}$ and dielectric permittivities $\varepsilon_{pq}^{(n),\xi}$ measured at strain ξ = const, where n=1 is related to FC and n=2 is related to polymer. Calculations of the effective electromechanical properties of the 1–3 composite are carried out within the framework of either the effective field method (EFM) or the finite element method (FEM), and some results are compared in this paper.

Based on the EFM concepts [5, 12, 18], one can describe an electromechanical interaction in the system "rods—matrix" (Fig. 1) using a local field that acts on each rod. This effective field is determined taking into account a system of the interacting piezo-active rods and boundary conditions concerned with the rod shape. The boundary conditions involve components of electric and mechanical fields at the rod—matrix interface. The 9×9 matrix characterising the electromechanical properties of each component (n=1 or 2) is written in the form [12, 18]

$$\left\|C^{(n)}\right\| = \begin{pmatrix} \left\|c^{(n),E}\right\| & \left\|e^{(n)}\right\|^t \\ \left\|e^{(n)}\right\| & \left\|-\varepsilon^{(n),\xi}\right\| \end{pmatrix}, \tag{2}$$

where the superscript t denotes the transposition. The effective electromechanical properties of the 1–3 composite are described by the 9×9 matrix

$$\|C^*\| = \left\|C^{(2)}\right\| + m\left(\left\|C^{(1)}\right\| - \left\|C^{(2)}\right\|\right) \left[\|I\| + (1-m)\|S\|\left\|C^{(2)}\right\|^{-1}\left(\left\|C^{(1)}\right\| - \left\|C^{(2)}\right\|\right)\right]^{-1}. \tag{3}$$

In Eq. (3), the matrices of the electromechanical constants $\left\|C^{(1)}\right\|$ and $\left\|C^{(2)}\right\|$ have a form that is shown in Eq. (2), m is the volume fraction of FC, $\|I\|$ is the identity matrix, and $\|S\|$ is the matrix that contains the Eshelby tensor components [22] depending on the elements of

$\|C^{(2)}\|$ and the rod shape [12, 18]. In our study, the ratio $\eta = a_2 / a_1$ of semiaxes of the ellipse in the rod cross section (see Fig. 1 and Eq. (1)) and the volume fraction m of FC are regarded as two independent parameters to be varied in ranges $0<\eta\leq 1$ and $0<m<\pi/4$, respectively. The limiting case of $\eta=0$ corresponds to the 2–2 parallel-connected composite, and the limiting case of $\eta=1$ is relevant to circular rod cross section of the 1–3 composite. The upper limit $m=\pi/4$ corresponds to the ratio of the area of the ellipse to the area of the rectangle on condition that this ellipse has been inscribed into the rectangle. This rectangle is regarded as a base of a representative unit cell [10, 14–16] of the 1–3 composite.

The prediction of the effective electromechanical properties in our work is also carried out using the FEM. It should be mentioned that in the last decades, the FEM has been applied to 1–3 FC / polymer composites with a periodic arrangement of the rods (see, *e.g.*, papers [10, 12, 14–16]). Following the FEM, the unit-cell model of the 1–3 composite with the regular arrangement of the rods (Fig. 1) is put forward, and periodic boundary conditions for the representative unit cell are considered. In the present work, the COMSOL package [23] is applied to obtain the volume-fraction dependence of the effective electromechanical properties. The rectangular unit cell, containing the FC rod in the form of the elliptic cylinder with semiaxes a_f (Fig. 1) adjusted to yield the appropriate volume fraction of FC, is discretised using triangular elements. The unknown displacement field is interpolated using second-order Lagrange shape functions, leading to a problem with approximately 120,000 to 200,000 degrees of freedom. The number of the degrees of freedom depends on the ratio of semiaxes η.

Periodicity is enforced at the boundary of the rectangular unit cell of the composite studied. The $\|C^*\|$ matrix of the effective electromechanical properties of the composite is computed column-wise, performing calculations for diverse average strain and electric fields imposed to the 1–3 structure with elliptic cylinders. The $\|C^*\|$ matrix has the form coinciding with that shown in Eq. (2). After solving the equilibrium problem, the effective elastic moduli $c^{*E}_{ab}(m,\eta)$, piezoelectric coefficients $e^*_{ij}(m,\eta)$ and dielectric permittivities $\varepsilon^{*\xi}_{pq}(m,\eta)$ of the composite studied are computed by means of averaging the resulting local stress and electric-displacement fields over the unit cell.

In both the aforementioned methods, other types of the piezoelectric coefficients (d^*_{ij}, g^*_{ij} and h^*_{ij}) are determined in the matrix form according to formulae [24] $\|d^*\| = \|e^*\| \times \|S^{*E}\|$, $\|g^*\| = \|\beta^{*\sigma}\| \times \|d^*\|$ and $\|h^*\| = \|\beta^{*\xi}\| \times \|e^*\|$, where $\|S^{*E}\| = \|c^{*E}\|^{-1}$ is the matrix of elastic compliances at electric field E = const, $\|\beta^{*\sigma}\| = \|\varepsilon^{*\sigma}\|^{-1}$ and $\|\beta^{*\xi}\| = \|\varepsilon^{*\xi}\|^{-1}$ are the matrices of dielectric impermeabilities at mechanical stress σ = const and strain ξ = const, respectively. In addition, electromechanical coupling factors

$$k^*_{3j} = d^*_{3j}\left(\varepsilon^{*\sigma}_{33} S^{*E}_{jj}\right)^{-1/2} \tag{4}$$

are calculated on the basis of effective constants from $\|d^*\|$, $\|\varepsilon^{*\sigma}\|$, and $\|S^{*E}\|$.

3 Piezoelectric response and anisotropy

Calculations are carried out using experimental room-temperature electromechanical constants of the FC and polymer components (Table 1). To show different variants of behaviour of the effective parameters of the 1–3 composite and variations of anisotropy of its piezoelectric properties, we consider the following examples of FC: the "soft" PCR-7 M composition based on Pb(Zr, Ti)O_3 with high piezoelectric and dielectric properties [25] and the

Table 1 Room-temperature elastic moduli $c^{(n),E}_{ab}$ (in 10^{10}Pa), piezoelectric coefficients $e^{(n)}_{3j}$ (in C / m^2) and dielectric permittivities $\varepsilon^{(n),\xi}_{33}/\varepsilon_0$ of FC and polymer components.

Components	$c^{(n),E}_{11}$	$c^{(n),E}_{12}$	$c^{(n),E}_{13}$	$c^{(n),E}_{33}$	$e^{(n)}_{31}$	$e^{(n)}_{33}$	$\varepsilon^{(n),\xi}_{33}/\varepsilon_0$
Poled FCs							
PCR-7M [25]	13.3	9.2	9.1	12.5	−9.5	31.1	1810
Modified $PbTiO_3$ [26]	14.33	3.221	2.417	13.16	0.459	6.50	133
Polymers							
75 / 25 mol. % copolymer of vinylidene fluoride and trifluoroethylene (VDF–TrFE) [3]	0.85	0.36	0.36	0.99	0.008	−0.29	6.0
Araldite [29]	0.78	0.44	0.44	0.78	0	0	4.0

1. PCR is the abbreviation for the group "piezoelectric ceramics from Rostov-on-Don", Russia [25]. The PCR-7 M FC has been manufactured by means of hot pressing. According to data from paper [30], this FC composition is characterised by the largest $e^{(1)}_{33}/c^{(1),E}_{33}$ ratio that promotes high piezoelectric sensitivity and large figures of merit of the 1–3 PCR-7M / polymer composites.

2. Modified $PbTiO_3$ is the $(Pb_{0.9625}La_{0.025})(Ti_{0.99}Mn_{0.01})O_3$ FC [26] manufactured by the conventional method.

"hard" modified $PbTiO_3$ composition with large anisotropy of the piezoelectric coefficients $d_{33}^{(1)}\Big/d_{31}^{(1)}$ and moderate piezoelectric and dielectric properties [26]. The importance of the anisotropy factor $d_{33}^{(1)}\Big/d_{31}^{(1)}$ in the $PbTiO_3$-type FCs and their advantages concerned with sensor, hydrophone and other piezotechnical applications were discussed in many papers (see, e,g., Refs. 27, 28). The FC components listed in Table 1 are also distinguished by signs and anisotropy of the piezoelectric coefficients $e_{3j}^{(1)}$. The following polymer components have been chosen: 75/25 mol. % copolymer of vinylidene fluoride and trifluoroethylene (VDF–TrFE) with considerable piezoelectric anisotropy [3], and araldite that is a piezo-passive material [29] with elastic properties that are not strongly different from those of VDF–TrFE (see Table 1).

As follows from an analysis of the $\|C^*(m,\eta)\|$ matrix of the effective electromechanical properties determined using Eq. (3), the 1–3 composite studied is characterised by *mm*2 symmetry. The corresponding matrix of the effective piezoelectric properties determined on the basis of Eq. (3) is

$$\|y^*\| = \begin{pmatrix} 0 & 0 & 0 & 0 & y_{15}^* & 0 \\ 0 & 0 & 0 & y_{24}^* & 0 & 0 \\ y_{31}^* & y_{32}^* & y_{33}^* & 0 & 0 & 0 \end{pmatrix},$$

where $y = d$, e, g, or h. Below we show some examples of behaviour of the piezoelectric coefficients y_{3j}^* relevant to the response of the composite along the axis OX_3 (*i.e.*, the poling axis of FC) or along the directions perpendicular to OX_3.

Due to the system of the long FC rods parallel to the OX_3 axis, the piezoelectric coefficients e_{3j}^* and h_{3j}^* show large anisotropy in wide m and η ranges. It means that inequalities $e_{33}^*\Big/\left|e_{31}^*\right| >> 1, e_{33}^*\Big/\left|e_{32}^*\right| >> 1, h_{33}^*\Big/\left|h_{31}^*\right| >> 1$, and $h_{33}^*\Big/\left|h_{32}^*\right| >> 1$ hold for different combinations of the components listed in Table 1 and—mainly—irrespectively of signs of the piezoelectric coefficients $e_{ij}^{(n)}$ of these components.

A comparison of the EFM calculation results with those obtained using the FEM is carried out for the piezoelectric coefficients d_{3j}^* of a series of composites with $0.01 \le \eta \le 1$ (Table 2). It is seen that the piezoelectric coefficients d_{3j}^* calculated by these methods are in good agreement in wide m and η ranges. Some deviations of results for d_{31}^* and d_{32}^*, especially at small η values (see Table 2), may be explained by an approximate character of averaging in the EFM. It seems to be probable that the effective field acting along the OX_1 and OX_2 axes (Fig. 1) at $\eta << 1$ is affected by curvature of rods more considerably than that accounted in the averaging procedure and Eq. (3). At the same time, values of the hydrostatic piezoelectric coefficient $d_h^* = d_{31}^* + d_{32}^* + d_{33}^*$ of the 1–3 composite agree in wide m and η ranges very well (see Table 2).

Approaching $\eta \to 1$ makes the aforementioned deviations (concerned with the OX_1 and OX_2 directions) slighter, as is shown in Table 2. In the limiting case of $\eta = 1$, results of both EFM and FEM calculations agree with data obtained using formulae [5] for the 1–3 composite with rods in the form of the circular cylinder: differences between the effective piezoelectric coefficients y_{3j}^* ($y = d$, e, g, or h) calculated for $0 < m \le 0.7$ do not exceed 1%. Table 3 contains data on the effective piezoelectric coefficients d_{3j}^* and e_{3j}^* of the composite with $\eta << 1$. In a limiting case of $\eta = 0$ (*i.e.*, $a_2 = 0$, see Fig. 1), this composite becomes laminar with 2–2 connectivity and interfaces $x_2 = \text{const}$. The effective electromechanical properties of the 2–2 composite are determined using the matrix method [29, 31] that allows for the electromechanical interaction between the piezo-active layers distributed regularly. Dependences of $d_{31}^*, d_{32}^*, e_{31}^*$, and e_{32}^* on η at $m = \text{const}$ (Table 3) suggest that only slight differences between the similar parameters take place at $\eta \le 10^{-3}$: at these aspect ratios the shape of the cross section of each rod (Fig. 1) changes insignificantly and there is no significant difference between the anisotropic piezoelectric properties of the 2–2 and 1–3 composites. Moreover, at $\eta \to 0$ results of EFM calculations correlate with evaluations performed on the basis of formulae [32] for the 2–2 parallel-connected composite. For example, differences between the effective electromechanical properties of the 1–3 composite at $\eta = 0.01$ and the related 2–2 composite are less than 5 %. The piezoelectric coefficients d_{33}^* and e_{33}^* which characterise the piezoelectric properties along the OX_3 axis remain almost constant in the whole range $0 \le \eta \le 1$ because the interfaces in the composite are parallel to the OX_3 axis irrespectively of the curvature of the rod base. This constancy is in agreement with recent data from work [14] on the longitudinal 1–3 composite poled along the OX_3 axis.

We note that the 1–3 composite at $\eta << 1$ and $m \ge 0.5$ shows an unusual piezoelectric anisotropy: according to data from Table 3, $d_{33}^*\Big/\left|d_{31}^*\right| \approx 10$ and $d_{33}^*\Big/\left|d_{32}^*\right| \approx 3.4 \ldots 4.7$. Surprisingly, such behaviour is observed in the presence of the modified $PbTiO_3$ FC component with $d_{33}^{(1)}\Big/\left|d_{31}^{(1)}\right| \approx 12$. The variations of the $d_{33}^*\Big/\left|d_{31}^*\right|$ and $d_{33}^*\Big/\left|d_{32}^*\right|$ ratios are mainly connected with elliptic cross section of the rod. Contrary to this microgeometric factor, the piezo-passive matrix surrounding the FC rods slightly influences the $d_{33}^*\Big/\left|d_{31}^*\right|$ and $d_{33}^*\Big/\left|d_{32}^*\right|$ ratios. Furthermore, at $0.1 < m < 0.4$ in this composite, a ratio $d_{32}^*\Big/d_{31}^{(1)} \approx 4$ is also explained by the presence of the cylindrical FC rods with $\eta << 1$. It should be added for comparison, that the related $PbTiO_3$-based composite with the FC rods in the form of circular cylinders [12] is characterised by a non-monotonic volume-fraction dependence of d_{31}^* with $\min d_{31}^*\Big/d_{31}^{(1)} = \min d_{32}^*\Big/d_{31}^{(1)} \approx 2$.

Table 2 Effective piezoelectric coefficients d^*_{3j} and d^*_h (in pC / N) of 1–3 PCR-7 M / polymer composites with η = const. Calculations have been made using either the EFM or the FEM.

η	m	d^*_{31}, EFM	d^*_{32}, EFM	d^*_{33}, EFM	d^*_h, EFM	d^*_{31}, FEM	d^*_{32}, FEM	d^*_{33}, FEM	d^*_h, FEM
1–3 PCR-7M / araldite composite									
0.01	0.01	−31.8	−25.6	75.9	18.5	−30.4	−26.4	76.0	19.2
	0.05	−120	−93.6	278	64.4	−111	−98.5	278	68.5
	0.10	−183	−141	416	92	−168	−150	417	99
	0.15	−222	−172	499	105	−203	−183	499	113
	0.20	−248	−194	554	112	−228	−207	555	120
	0.30	−282	−226	623	115	−260	−241	623	122
	0.50	−316	−269	692	107	−300	−285	692	107
	0.70	−333	−303	727	91	−326	−317	726	83
0.05	0.01	−30.2	−26.6	76.0	19.2	−29.9	−26.7	76.0	19.4
	0.05	−114	−97.0	278	67.0	−110	−99.0	278	69.0
	0.10	−175	−146	416	95	−167	−151	417	99
	0.15	−214	−176	499	109	−202	−184	499	113
	0.20	−241	−198	554	115	−227	−207	555	121
	0.30	−276	−229	623	118	−259	−241	623	123
	0.50	−313	−272	692	107	−298	−286	692	108
	0.70	−332	−303	725	90	−325	−317	726	84
0.10	0.01	−29.4	−27.1	76.1	19.6	−29.4	−27.1	76.1	19.6
	0.05	−111	−99.0	278	68.0	−109	−99.7	278	69.3
	0.10	−170	−149	417	98	−166	−151	417	100
	0.15	−209	−180	499	110	−201	−184	499	114
	0.20	−235	−202	554	117	−225	−208	555	122
	0.30	−271	−233	623	119	−258	−242	623	123
	0.50	−309	−274	692	109	−297	−286	692	109
	0.70	−330	−306	727	91	−323	−317	726	86
0.50	0.01	−28.3	−27.8	76.1	20.0	−28.3	−27.8	76.1	20.0
	0.05	−105	−103	278	70	−105	−103	278	70
	0.10	−160	−155	417	102	−160	−156	417	101
	0.15	−196	−188	500	116	−195	−189	500	116
	0.20	−221	−212	555	122	−220	−213	555	122
	0.30	−255	−244	623	124	−253	−246	623	124
	0.50	−296	−284	692	112	−292	−289	692	111
	0.70	−322	−313	727	92	−320	−319	726	87
1	0.01	−28.0	−28.0	76.1	20.1	−28.0	−28.0	76.1	20.1
	0.05	−104	−104	278	70	−104	−104	278	70
	0.10	−158	−158	417	101	−158	−158	417	101
	0.15	−192	−192	500	116	−192	−192	500	116
	0.20	−216	−216	555	123	−216	−216	555	123
	0.30	−249	−249	623	125	−249	−249	623	125
	0.50	−290	−290	692	112	−290	−290	692	112
	0.70	−317	−317	727	93	−319	−319	726	93
1–3 PCR-7M / VDF-TrFE composite with $\boldsymbol{P}_r^{(2)} \uparrow \downarrow OX_3$									
0.01	0	−12.0	−12.0	38.0	14.0	−12.0	−12.0	38.0	14.0
	0.01	−29.3	−24.4	82.6	28.9	−28.0	−24.9	82.7	29.8
	0.05	−87.0	−63.3	222	71.7	−78.2	−67.1	223	77.7
	0.10	−140	−97.7	340	102	−123	−105	341	113
	0.15	−179	−124	422	119	−156	−135	423	132
	0.20	−208	−145	483	130	−182	−159	484	143

Table 2 (continued).

η	m	d_{31}^*, EFM	d_{32}^*, EFM	d_{33}^*, EFM	d_h^*, EFM	d_{31}^*, FEM	d_{32}^*, FEM	d_{33}^*, FEM	d_h^*, FEM
	0.30	−250	−180	566	136	−221	−197	567	149
	0.50	−297	−236	659	126	−275	−256	660	129
	0.70	−324	−283	710	103	−314	−301	710	95
0.05	0	−12.0	−12.0	38.0	14.0	−12.0	−12.0	38.0	14.0
	0.01	−28.0	−24.9	82.7	29.8	−27.7	−25.0	82.8	30.1
	0.05	−82.0	−65.6	222	74.4	−77.6	−67.4	223	78.0
	0.10	−132	−101	340	107	−122	−106	341	113
	0.15	−170	−128	422	124	−155	−135	423	133
	0.20	−200	−149	483	134	−181	−159	484	144
	0.30	−242	−184	566	140	−220	−198	567	149
	0.50	−293	−238	660	129	−273	−256	660	131
	0.70	−322	−284	711	105	−312	−301	710	97
0.10	0	−12.0	−12.0	38.0	14.0	−12.0	−12.0	38.0	14.0
	0.01	−27.4	−25.2	82.8	30.2	−27.3	−25.3	82.8	30.2
	0.05	−78.9	−67.1	222	76.0	−76.7	−67.9	223	78.4
	0.10	−127	−104	341	110	−121	−106	341	114
	0.15	−164	−131	423	128	−154	−136	423	133
	0.20	−193	−153	483	137	−180	−160	484	144
	0.30	−236	−188	566	142	−219	−199	567	149
	0.50	−288	−241	660	131	−272	−257	660	131
	0.70	−319	−286	711	106	−311	−302	710	97
0.50	0	−12.0	−12.0	38.0	14.0	−12.0	−12.0	38.0	14.0
	0.01	−26.3	−25.8	82.9	30.8	−26.3	−25.8	82.9	30.8
	0.05	−72.9	−70.2	223	79.9	−72.8	−70.3	223	79.9
	0.10	−116	−110	341	115	−115	−110	341	116
	0.15	−148	−140	423	135	−147	−140	423	136
	0.20	−175	−163	484	146	−173	−165	484	146
	0.30	−215	−200	567	152	−212	−203	567	152
	0.50	−271	−254	660	135	−265	−260	660	135
	0.70	−308	−296	711	107	−306	−303	710	101
1	0	−12.0	−12.0	38.0	14.0	−12.0	−12.0	38.0	14.0
	0.01	−26.0	−26.0	82.9	30.9	−26.0	−26.0	82.9	30.9
	0.05	−71.4	−71.4	223	80.2	−71.4	−71.4	223	80.2
	0.10	−113	−113	341	115	−113	−113	341	115
	0.15	−144	−144	424	136	−144	−144	424	136
	0.20	−169	−169	484	146	−169	−169	484	146
	0.30	−207	−207	567	153	−207	−207	567	153
	0.50	−262	−262	660	136	−262	−262	660	136
	0.70	−302	−302	711	107	−305	−305	710	100

In the 1–3 PCR-7M / araldite composite $d_{3j}^* = 0$ and $d_h^* = 0$ at $m = 0$ irrespectively of η.

Now we give four examples of dependences of the piezoelectric properties on m and η at the following combinations of the components: PCR-7M / araldite (composite I), modified $PbTiO_3$ / araldite (composite II), PCR-7M / VDF–TrFE with $\boldsymbol{P}_r^{(2)} \uparrow\downarrow OX_3$ (composite III), and modified $PbTiO_3$ / VDF–TrFE with $\boldsymbol{P}_r^{(2)} \uparrow\downarrow OX_3$ (composite IV). It is assumed that the FC rods and the polymer matrix in composites III and IV are poled antiparallel. Such a variance of poling is possible due to the considerable difference [20, 21, 25] between the coercive fields of the FC and polymer components. It is noteworthy that the opposite poling directions of the components enable us to attain a more considerable piezoelectric activity of the 1–3 composite due to the

Table 3 Effective piezoelectric coefficients d_{3j}^* (in pC / N) and e_{3j}^* (in C / m^2) of modified $PbTiO_3$ / araldite composites with η=0 (2–2 connectivity) or η>0 (1–3 connectivity). Calculations have been made using either the matrix method (for η=0) or the EFM (for η>0).

m	d_{31}^*, η=0	d_{31}^*, $\eta=10^{-3}$ 10	d_{31}^*, $\eta=10^{-2}$	d_{32}^*, η=0	d_{32}^*, $\eta=10^{-3}$	d_{32}^*, $\eta=10^{-2}$	d_{33}^*, η=0	d_{33}^*, $\eta=10^{-3}$	d_{33}^*, $\eta=10^{-2}$
0.1	−5.39	−5.55	−6.32	−15.9	−16.5	−16.1	37.2	37.7	37.8
0.2	−5.11	−5.20	−5.75	−17.6	−18.1	−17.8	43.8	44.1	44.1
0.3	−4.89	−4.95	−5.33	−17.1	−17.6	−17.3	46.5	46.7	46.7
0.4	−4.75	−4.79	−5.05	−15.8	−16.2	−16.0	48.0	48.2	48.2
0.5	−4.64	−4.67	−4.86	−14.2	−14.5	−14.4	49.0	49.1	49.1
0.6	−4.57	−4.59	−4.72	−12.4	−12.7	−12.6	49.6	49.7	49.7
0.7	−4.51	−4.53	−4.61	−10.5	−10.7	−10.6	50.1	50.2	50.2

m	10^2 e_{31}^*, η=0	10^2 e_{31}^*, $\eta=10^{-6}$ 10	$10^2 e_{31}^*$, $\eta=10^{-3}$	$10^3 e_{32}^*$, η=0	$10^3 e_{32}^*$, $\eta=10^{-6}$	10^3 e_{32}^*, $\eta=10^{-3}$	e_{33}^*, η =0	e_{33}^*, $\eta=10^{-6}$	e_{33}^*, $\eta=10^{-3}$
0.1	3.70	3.70	3.56	2.83	2.76	2.80	0.644	0.644	0.644
0.2	7.41	7.42	7.17	6.31	6.16	6.24	1.29	1.29	1.29
0.3	11.1	11.2	10.8	10.7	10.7	10.6	1.93	1.93	1.93
0.4	14.9	14.9	14.5	16.4	16.4	16.2	2.58	2.58	2.58
0.5	18.7	18.7	18.3	24.2	24.2	23.9	3.22	3.22	3.22
0.6	22.6	22.6	22.2	35.4	35.4	34.9	3.86	3.86	3.86
0.7	26.6	26.6	26.3	52.8	52.8	52.0	4.51	4.51	4.51

following signs of the piezoelectric coefficients: $\mathrm{sgn}e_{31}^{(n)} = \mathrm{sgn}d_{31}^{(n)} < 0$ and $\mathrm{sgn}e_{33}^{(n)} = \mathrm{sgn}d_{33}^{(n)} > 0$.

Features of behaviour of the piezoelectric coefficients d_{3j}^* and g_{3j}^* in composites I–IV are shown in Figs. 2, 3, 4, 5 and 6[1]). According to formulae [24], d_{3j}^* and g_{3j}^* of the composite with *mm*2 symmetry are represented as follows:

$$d_{31}^* = e_{31}^* S_{11}^{*E} + e_{32}^* S_{12}^{*E} + e_{33}^* S_{13}^{*E}, \tag{5}$$

$$d_{32}^* = e_{31}^* S_{12}^{*E} + e_{32}^* S_{22}^{*E} + e_{33}^* S_{23}^{*E}, \tag{6}$$

$$d_{33}^* = e_{31}^* S_{13}^{*E} + e_{32}^* S_{23}^{*E} + e_{33}^* S_{33}^{*E}, \tag{7}$$

and

$$g_{3j}^* = d_{3j}^* \Big/ \varepsilon_{33}^{*\sigma} \tag{8}$$

(j=1, 2 and 3). In composites I–IV, d_{3j}^* and e_{3j}^* mainly show monotonic behaviour on η at m = const. The presence of interfaces parallel to the poling axis OX_3 of the 1–3 composite favours monotonic behaviour of the piezoelectric coefficients e_{3j}^* linking the piezoelectric polarisation $P^* \| OX_3$ and the mechanical strain ξ_j of the composite. Moreover, changes in semiaxes a_f (Fig. 1) would not give rise to a considerable change in the balance of items from Eqs. (5–7), and we see that all the piezoelectric coefficients depend on η at m = const almost monotonically (Figs. 2, 3, 4 and 5).

The non-monotonic volume-fraction dependences of d_{31}^* and d_{32}^* at η=const are predicted for the $PbTiO_3$-based composites irrespectively of the polymer matrix (see Fig. 3a and b as well as Fig. 5a and b). As follows from Table 1, elastic moduli $c_{ab}^{(1),E}$ of modified $PbTiO_3$ FC show an anisotropy that differs from the elastic anisotropy of polymers. For example, ratios $c_{11}^{(1),E} \Big/ c_{12}^{(1),E} = 4.4$ and $c_{11}^{(1),E} \Big/ c_{13}^{(1),E} = 5.9$ hold for modified $PbTiO_3$ FC, but elastic moduli $c_{ab}^{(2),E}$ of VDF–TrFE obey condition $c_{11}^{(2),E} \Big/ c_{12}^{(2),E} = c_{11}^{(2),E} \Big/ c_{13}^{(2),E} = 2.4$. The anisotropy of elastic moduli $c_{ab}^{(1),E}$ of modified $PbTiO_3$ FC considerably influence the balance of items that contain elastic compliances S_{11}^{*E}, S_{12}^{*E} and S_{22}^{*E} in Eqs. (5) and (6). Obviously, the elastic compliances with such subscripts describe the response of the composite along the axes of the ellipse (Fig. 1), and changes in the volume fraction m (*i.e.*, changes

[1] Volume-fraction dependences of g_{3j}^* are graphically represented in the range $0 \le m \le 0.2$ (Figs. 2, 3, 4, 5, and 6). A further increase of the volume fraction m at η = const leads to monotonic decreasing $\left|g_{3j}^*\right|$ only. So long as the $g_{3j}^{(2)}$ values of FCs are much times less than $\max\left|g_{3j}^*\right|$, we do not show "tails" of the volume-fraction dependences of g_{3j}^* at m>0.2.

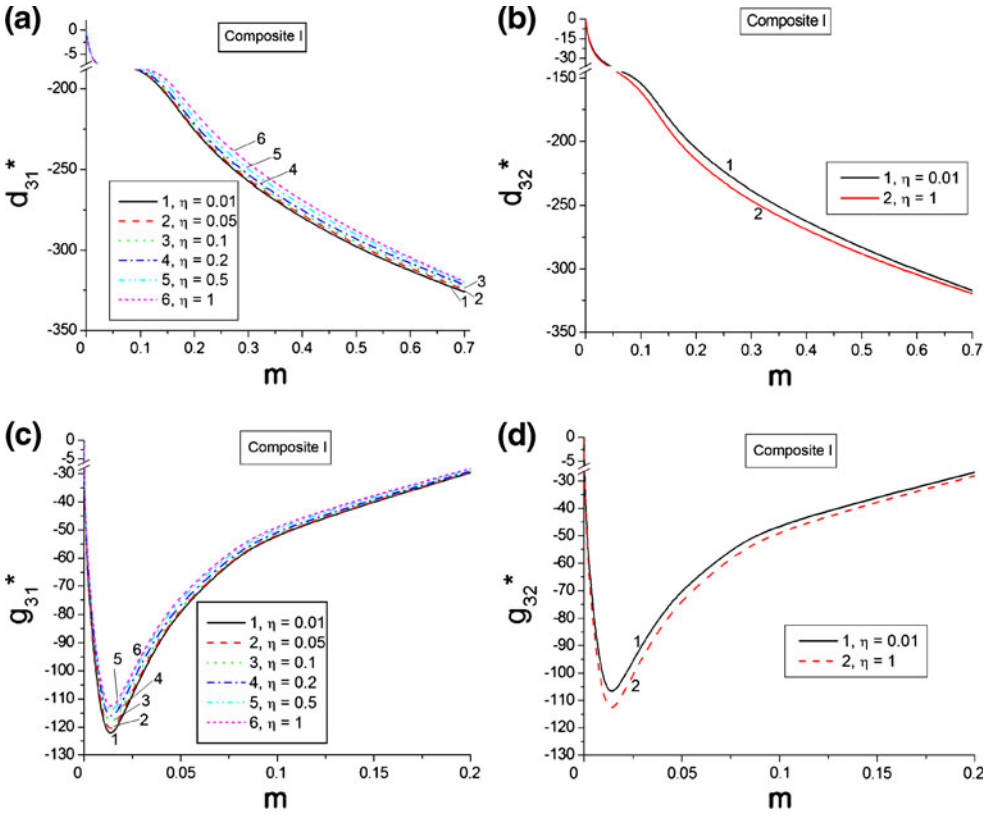

Fig. 2 Effective piezoelectric coefficients $d_{3j}^*(m,\eta)$ (in pC / N) and $g_{3j}^*(m,\eta)$ (in mV·m / N) of the 1–3 PCR-7M / araldite composite. Calculations have been made using the FEM

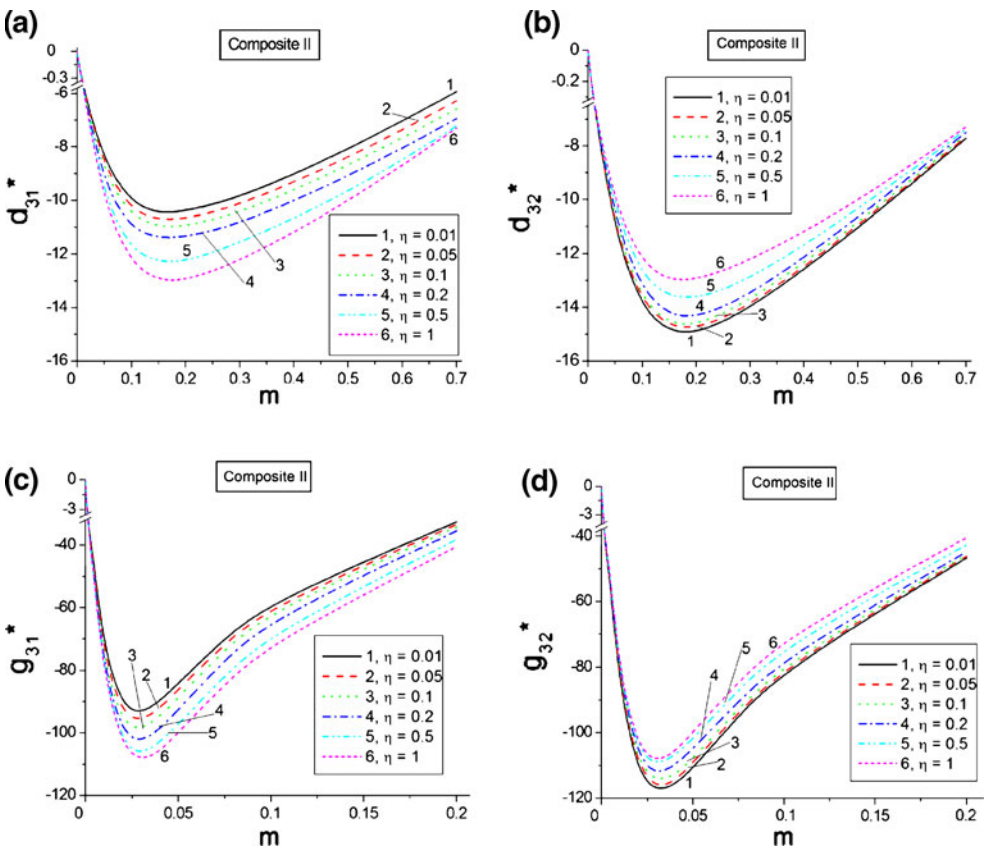

Fig. 3 Effective piezoelectric coefficients $d_{3j}^*(m,\eta)$ (in pC / N) and $g_{3j}^*(m,\eta)$ (in mV·m / N) of the 1–3 modified $PbTiO_3$ / araldite composite. Calculations have been made using the FEM

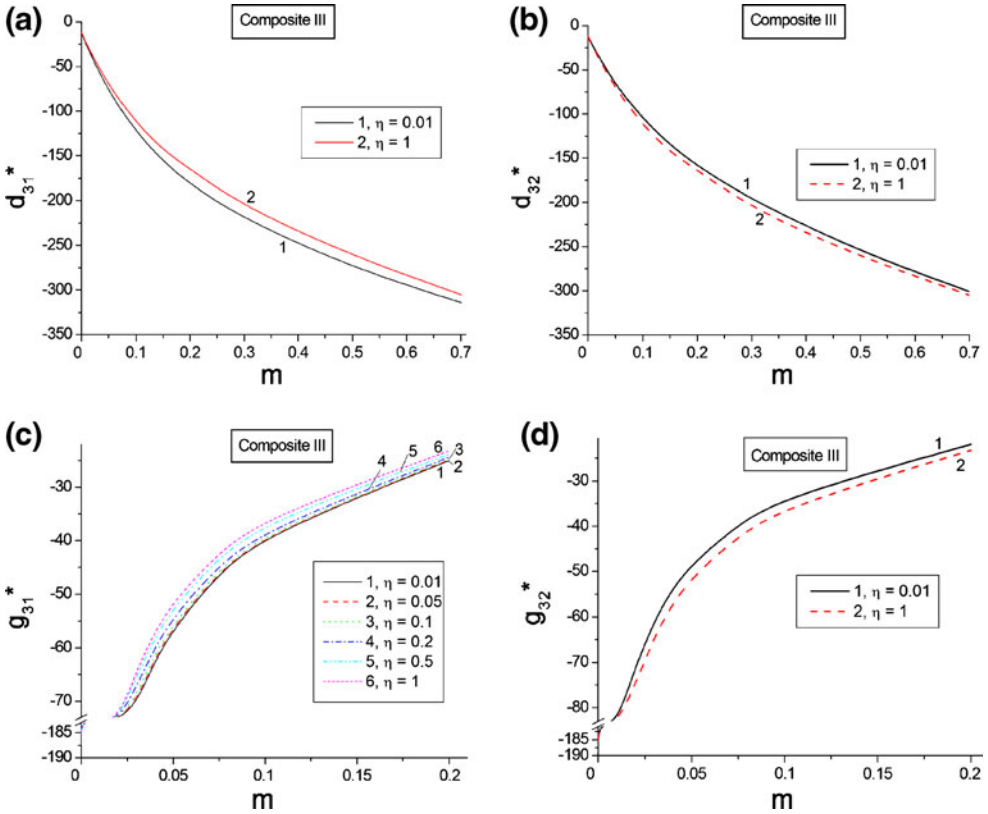

Fig. 4 Effective piezoelectric coefficients $d^*_{3j}(m,\eta)$ (in pC / N) and $g^*_{3j}(m,\eta)$ (in mV·m / N) of the 1–3 PCR-7M / VDF–TrFE composite with $\boldsymbol{P}_r^{(2)} \uparrow\downarrow OX_3$. Calculations have been made using the FEM

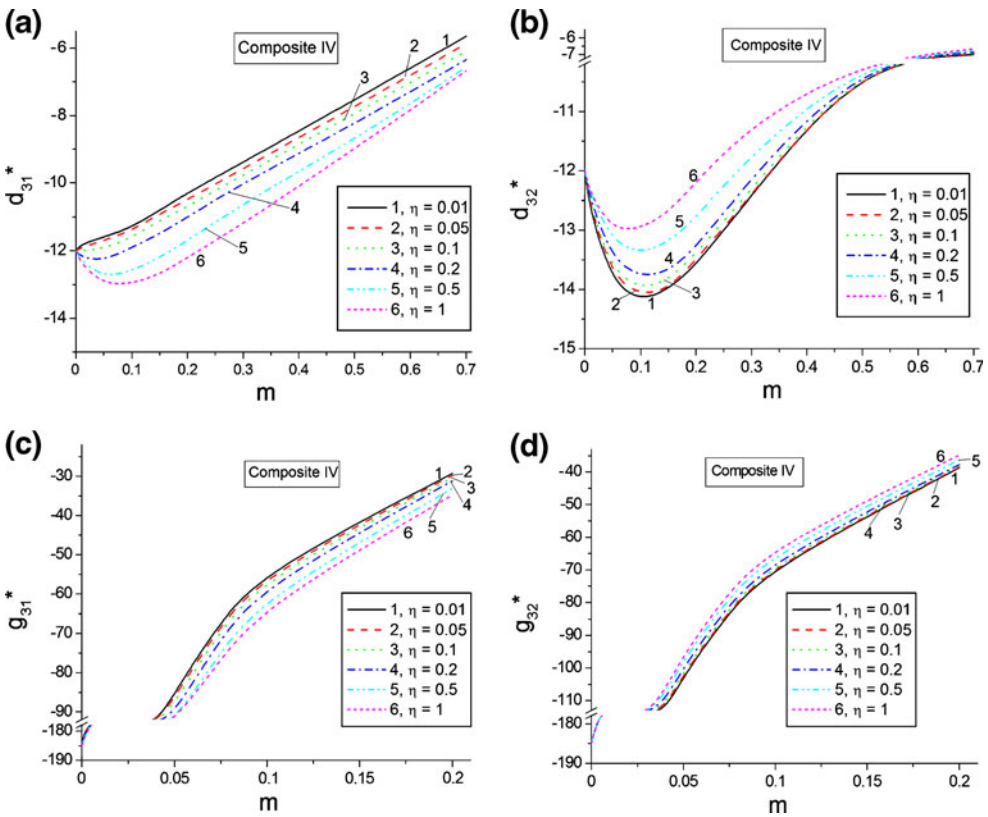

Fig. 5 Effective piezoelectric coefficients $d^*_{3j}(m,\eta)$ (in pC / N) and $g^*_{3j}(m,\eta)$ (in mV·m / N) of the 1–3 modified $PbTiO_3$ / VDF–TrFE composite with $\boldsymbol{P}_r^{(2)} \uparrow\downarrow OX_3$. Calculations have been made using the FEM

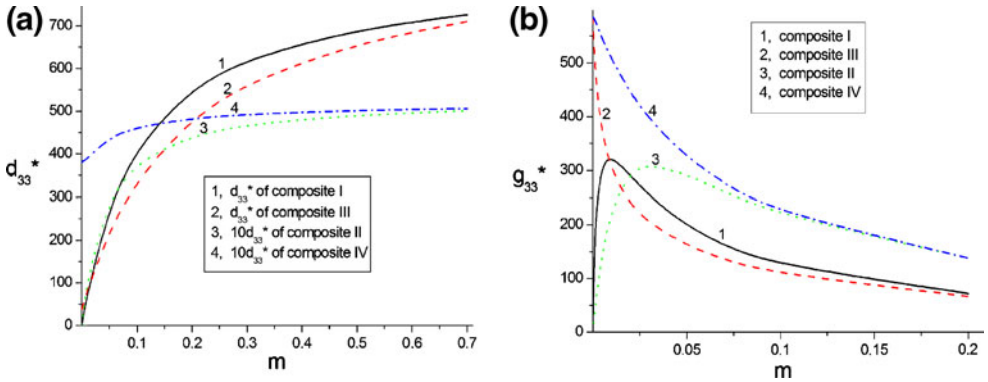

Fig. 6 Effective piezoelectric coefficients $d_{33}^*(m)$ (in pC / N) and $g_{33}^*(m)$ (in mV·m / N) of the 1–3 FC / polymer composites at $0<\eta\leq 1$. Calculations have been made using the FEM

in the area occupied by the ellipses in the X_1OX_2 plane in Fig. 1) would lead to changes in elastic and piezoelectric properties in accordance with Eqs. (5) and (6). In contrast to d_{31}^* and d_{32}^*, the monotonic behaviour of d_{33}^* in composites I – IV (Fig. 6) is accounted for by slight changes in the balance of items from Eq. (7). These items contain elastic compliances S_{13}^{*E}, S_{23}^{*E} and S_{33}^{*E}, which are related to the OX_3 axis being parallel to the rod interfaces in the 1–3 composite. We add that the piezoelectric response of the 1–3 composite along the OX_3 axis on loading in the same direction does not depend on the on the ratio of semiaxes η (*i.e.*, data from Fig. 7 hold at $0<\eta\leq 1$), and this performance is agreement with recent results [14].

The piezoelectric coefficients g_{3j}^* from Eq. (8) show non-monotonic behaviour in composites I and II (Figs. 2c, d, 3c, and d) with the piezo-passive polymer matrix. A monotonic increase in dielectric permittivity $\varepsilon_{33}^{*\sigma}$ of the composite on increasing m (see Eq. (8)) in combination with an appreciable increase in $\left|d_{3j}^*\right|$ at $m<<1$ (see, *e.g.*, Fig. 6a) promotes an appearance of extreme points of g_{3j}^* at almost equal volume fractions m (compare, *e.g.*, data from Fig. 2c, d and curve 1 in Fig. 6b). Due to the combination of the "soft" FC and the piezo-passive polymer, composite I shows the largest values of $\max\left|g_{3j}^*\right|\Big/g_{31}^{(1)}$: for example, at $0.01\leq\eta<0.1$ we have $\max\left|g_{31}^*\right|\Big/g_{33}^{(1)}\approx 17, \max\left|g_{32}^*\right|\Big/g_{32}^{(1)}=\max\left|g_{32}^*\right|\Big/g_{31}^{(1)}\approx 14$ and $\max g_{33}^*\Big/g_{33}^{(1)}\approx 19$. We see that η influences the aforementioned ratios slightly, and it may be concerned with microgeometry of the 1–3 composite as a whole. The presence of the piezo-active VDF–TrFE matrix with considerable $g_{3j}^{(2)}$ values becomes a factor that strongly influences the volume-fraction dependence of g_{3j}^* in composites III and IV (Fig. 4c and d, Fig. 5c and d, and curves 2 and 4 in Fig. 6). In this connection, the large piezoelectric sensitivity of composites III and IV might be exploited at the volume fractions of FC $m<0.05$, *i.e.*, at a moderate decrease in the $\left|g_{3j}^*\right|$ values. As for the the ratio of semiaxes η, it influences the piezoelectric coefficients g_{31}^* and g_{32}^* because of their link to d_{31}^* and d_{32}^*, respectively (see Eq. (8)). For the studied 1–3 composite with $mm2$ symmetry, the relation $d_{33}^*/d_{3k}^*=g_{33}^*/g_{3k}^*$, that characterizes piezoelectric anisotropy, holds at $k=1$ and 2, and no additional influence of dielectric permittivity $\varepsilon_{33}^{*\sigma}$ is to be taken into account.

We also consider the volume-fraction dependence of electromechanical coupling factors k_{3j}^* from Eq. (4) at η = const (Fig. 7). Calculations were made for composites III and IV with the piezo-active polymer matrix. Monotonic behaviour of $k_{3j}^*(m)$ takes place in both cases, irrespectively

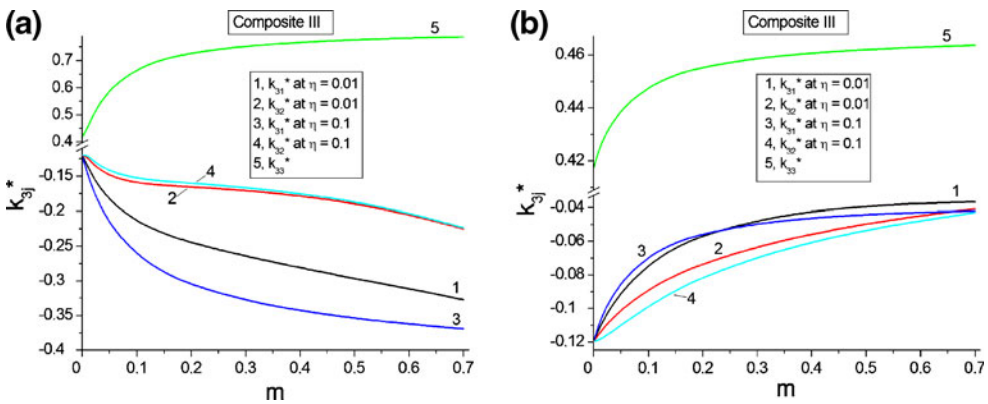

Fig. 7 Electromechanical coupling factors $k_{3j}^*(m)$ of the 1–3 PCR-7M / VDF–TrFE composite with $\boldsymbol{P}_r^{(2)}\uparrow\downarrow OX_3$ at η=0.01 and η=0.1. Calculations have been made using the EFM

of peculiarities of $d_{3j}^*(m)$ (cf. Figs. 7a and 4a, b or Figs. 7b and 5a, b) and changes in the aspect ratio η. Dielectric permittivity $\varepsilon_{33}^{*\sigma}(m)$ increases monotonically at various η, It seems reasonable to assume that changes in elastic compliances $S_{jj}^{*E}(m)$ strongly influence the balance of electromechanical constants in Eq. (4) and promote the monotonic dependence of $k_{3j}^*(m)$ in the composites based on FC with various piezoelectric anisotropy. In composite IV conditions $k_{33}^*/|k_{31}^*| > 5$ and $k_{33}^*/|k_{32}^*| > 5$ are satisfied in wide volume-fraction ranges (Fig. 7b) due to the presence of the FC and polymer components with large anisotropy of the piezoelectric coefficients $d_{3j}^{(n)}$.

4 Conclusions

In this paper, we have predicted and analysed the effective piezoelectric properties of the 1–3 FC / polymer composites with rods in the form of elliptic cylinders. In contrast to the well-known transversely isotropic 1–3 composites [2–5, 8–10], the composites studied in this work are characterised by *mm*2 symmetry and certain anisotropy of the effective electromechanical properties. In this connection, the aspect ratio η is to be regarded as an important factor that influences the anisotropy of the piezoelectric coefficients of the studied composites. The presence of the elliptic configuration of cross section of the rod (Fig. 1) and components with various piezoelectric activity enables to vary the piezoelectric anisotropy in such a way that has no analogs among the piezo-active composites studied earlier. The effective piezoelectric coefficients calculated within the framework of the EFM are in good agreement with the similar piezoelectric coefficients predicted using the FEM.

The results of the present study can be taken into account for the manufacture and design of the novel anisotropic 1–3 composites. Describing the role of the FC rod shape factor (aspect ratio η) in influencing the piezoelectric anisotropy of the studied composites, we conclude that the piezoelectric coefficient d_{33}^* is not influenced, but d_{31}^* and d_{32}^* are significantly influenced by the factor η, at least for composites II and IV (see Figs. 3a, b and 5a, b). It is clear that due to the microgeometric feature of the 1–3 composite (Fig. 1), the influence of η on d_{31}^* is opposite to the one on d_{32}^*, so that in applications involving one of these piezoelectric coefficients (either d_{31}^* or d_{32}^*), the orientation of the FC rods in the composite sample can be suitably arranged.

The 1–3 composites considered in the present paper show good performance. For example, $|d_{3j}^*| > 100\text{pC/N}$ (Table 2, Figs. 2a, b, 4a, b, and 6a), $d_h^* > 100\text{pC/N}$ (Table 2) are important parameters for actuators and hydrophones. The anisotropy factor $d_{33}^*/|d_{31}^*| \approx 10$ (Table 3, Figs. 3a, b, 5a, b, and 6a) is to be taken into account when creating sensors and acoustic antennae. Values of $|g_{3j}^*| > 100\ \text{mV} \cdot \text{m/N}$ (Figs. 2c, d, 3c, d, 4c, d, 5c, d, and 6b) are of interest for sensor and hydrophone applications. The large values of the electromechanical coupling factors k_{3j}^* (Fig. 7a) are important for transducer applications. The presence of the extreme points of the piezoelectric coefficients d_{3j}^*, d_h^* and g_{3j}^* and the information on the location of these extreme points (volume fraction m, aspect ratio η *etc*.) are of benefit for the optimisation and exploitation of the effective properties of the composites studied in this work.

Acknowledgments The authors would like to thank Prof. Dr. A. V. Turik and Prof. Dr. A. E. Panich (Southern Federal University, Rostov-on-Don, Russia) and Dr. C. R. Bowen (University of Bath, Bath, UK) for their interest in the research problems. Financial support by the University of Rome "Tor Vergata" (Rome, Italy) for the stay and research of one of the authors (V. Yu. T.) is also gratefully acknowledged.

References

1. T.R. Gururaja, A. Safari, R.E. Newnham, L.E. Cross, in *Electronic ceramics: properties, devices, and applications*, ed. by M. Levinson (Marcel Dekker, New York, Basel, 1988), pp. 92–128
2. H.L.W. Chan, J. Unsworth, IEEE Trans. Ultrason. Ferroelect., a Freq. Control **36**, 434–441 (1989)
3. H. Taunaumang, I.L. Guy, H.L.W. Chan, J. Appl. Phys. **76**, 484–489 (1994)
4. O. Sigmund, S. Torquato, I.A. Aksay, J. Mater. Res. **13**, 1038–1048 (1998)
5. A.A. Grekov, S.O. Kramarov, A.A. Kuprienko, Mech. Compos. Mater. **25**, 54–61 (1989)
6. R.E. Newnham, D.P. Skinner, L.E. Cross, Mater. Res. Bull. **13**, 525–536 (1978)
7. W.A. Smith, IEEE Trans. Ultrason., Ferroelect., a. Freq. Control **30**, 41–49 (1993)
8. H. Jensen, IEEE Trans. Ultrason., Ferroelect., a. Freq. Control **38**, 591–594 (1991)
9. C. Poizat, M. Sester, Comput. Mater Sci. **16**, 89–97 (1999)
10. H. Berger, S. Kari, U. Gabbert, R. Rodríguez-Ramos, J. Bravo-Castillero, R. Guinovart-Díaz, Mater. Sci. Eng. A **412**, 53–60 (2005)
11. R. Kar-Gupta, T.A. Venkatesh, Acta Mater. **55**, 1093–1108 (2006)
12. V.Yu. Topolov, P. Bisegna, A.V. Krivoruchko, J. Phys. D: Appl. Phys. **41**, 035406 – 8 p. (2008)
13. K.Y. Hashimoto, M. Yamaguchi, In: Proc. IEEE Ultrason. Symp., Williamsburg, Va, Nov. 17–19, 1986. V. 2 (New York, NY), 697–702 (1986)
14. R. Kar-Gupta, C. Marcheselli, T.A. Venkatesh, J. Appl. Phys. **104**, 024105–17 p. (2008)
15. E.C. Nelli Silva, J.S. Ono Fonseca, N. Kikuchi, Comput. Mech. **19**, 397–410 (1997)
16. H.E. Pettermann, S. Suresh, Internat. J. Solids a. Struct. **37**, 5447–5464 (2000)
17. J.G. Wan, B.Q. Tao, Mater. Design **21**, 533–536 (2000)
18. A.V. Krivoruchko, V. Yu. Topolov, Nano- i Mikrosistemnaya Tekhnika Nr. **7**, 35–39 (2006), in Russian
19. A. Safari, E.K. Akdogan, Ferroelectrics **331**, 153–179 (2006)

20. K.L. Ng, H.L.W. Chan, C.L. Choy, IEEE Trans. Ultrason., Ferroelect., a. Freq. Control **47**, 1308–1315 (2000)
21. G.M. Sessler, J. Acoust, Soc. Am. **70**, 1596–1608 (1981)
22. L.-P. Chao, J.H. Huang, J. Appl, Phys. **85**, 6695–6703 (1999)
23. COMSOL, Inc. 2007 *COMSOL Multiphysics™ User's Guide* (version 3.3a), http://www.comsol.com/
24. T. Ikeda, *Fundamentals of piezoelectricity* (Oxford University Press, Oxford, New York, Toronto, 1990)
25. A. Ya. Dantsiger, O.N. Razumovskaya, L.A. Reznitchenko, L.D. Grineva, R.U. Devlikanova, S.I. Dudkina, S.V. Gavrilyatchenko, N.V. Dergunova, A.N. Klevtsov, Highly Effective Piezoceramic Materials (Handbook) (Kniga, Rostov-on-Don, in Russian) (1994)
26. S. Ikegami, I. Ueda, T. Nagata, J. Acoust, Soc. Am. **50**, 1060–1066 (1971)
27. D. Damjanovic, T.R. Gururaja, L.E. Cross, Am. Cer. Soc. Bull. **66**, 699–703 (1987)
28. A.V. Turik, V. Yu. Topolov, J. Phys, D: Appl. Phys. **30**, 1541–1549 (1997)
29. F. Levassort, M. Lethiecq, D. Certon, F. Patat, IEEE Ultrason., Ferroelect., a. Freq. Contr. **44**, 445–452 (1997)
30. VYu Topolov, A.V. Turik, Tech. Phys. **46**, 1093–1100 (2001)
31. F. Levassort, V. Yu. Topolov, M. Lethiecq, J. Phys, D: Appl. Phys. **33**, 2064–2068 (2000)
32. A.A. Grekov, S.O. Kramarov, A.A. Kuprienko, Ferroelectrics **76**, 43–48 (1987)